



# Enhanced understanding on incipient sediment motion and sediment suspension through oscillating-grid turbulence experiments\*

Wan Hanna Melini WAN MOHTAR

(Department of Civil & Structural Engineering, University Kebangsaan Malaysia, Bandar Baru Bangi 43600, Malaysia)

E-mail: hanna@ukm.edu.my

Received Oct. 6, 2016; Revision accepted Jan. 13, 2017; Crosschecked Oct. 10, 2017

**Abstract:** Sediment dynamics are usually described in terms of the studies developed under a steady uniform flow, where the hydrodynamic forces are taken those pertaining to the mean time-averaged flow speed. However, the inherent turbulence plays an important role and should be considered implicitly in describing the complexity of turbulence effects in geophysical phenomena. This paper reviews the implementation of isolated turbulence, generated by oscillating grid on two important sediment transport phenomena, i.e., incipient sediment motion and suspension. The generated quasi-isotropic, laterally homogenous turbulence (that is, at a distance further away from the grid) permits an in-depth investigation of the effect of turbulent fluctuations and brings new insights in understanding both phenomena. The critical Shields profile for the incipient sediment motion characterized using the second order of turbulence statistics is qualitatively similar to the Shields curve obtained under a steady uniform flow. In the suspension of particles, there is a two-way interaction between sediment and turbulence. High concentration of suspended particles changes the turbulence structure and the presence of coherent vortices changes the particle settling velocity, which subsequently alters the concentration within the suspension layer. The studies of turbulence on incipient sediment motion and particle suspension provide a better understanding of the underlying physics of sediment behavior at the near-bed region.

**Key words:** Oscillating-grid turbulence; Incipient sediment motion; Sediment resuspension

<http://dx.doi.org/10.1631/jzus.A1600659>

**CLC number:** TV14

## 1 Introduction

The action of the bottom shear stress at the bed of a water stream induces several sediment-related phenomena such as incipient sediment motion and sediment resuspension or entrainment. Once the sediment is moved or entrained, it is transported either as bedload or suspension, and may cause disturbance

to the bed morphology and water quality through erosion and sedimentation processes. This collective movement of solid particles is a rather complex problem, not only due to the dual interaction of sediment and the changes of flow, but also the effect of the generation and migration of bed forms. Numerous studies have focused on the complexity of flow-sediment interaction in a uniform steady channel flow, where the fluctuating bottom shear stresses are correlated with the time-averaged mean flow speed and the effect of turbulence is considered implicitly (Shvidchenko and Pender, 2000; Rijn, 2007; Lamb *et al.*, 2008; Srinivasan *et al.*, 2008; Parker *et al.*,

\* Project supported by the Dana Impak Perdana (No. DIP-2015-006) and Arus Perdana (No. AP-2014-008), Universiti Kebangsaan Malaysia

ORCID: Wan Hanna Melini WAN MOHTAR, <http://orcid.org/0000-0002-5684-5577>

©Zhejiang University and Springer-Verlag GmbH Germany 2017

2011).

However, naturally occurring flows are neither uniform nor statistically stationary, with the turbulence intensity varying significantly both spatially and temporally. Typical factors causing this non-uniformity and/or intermittency can include local variations in bed slope or bed geometry, obstacles within the flow and the presence or development of intermittent coherent vortex structures in the near-bed region (Kaftori *et al.*, 1995; Nelson *et al.*, 1995; Niño and Garcia, 1996; Sumer *et al.*, 2003). Under these conditions, the near-bed turbulence is no longer necessarily correlated with the mean flow characteristics, and so the parametric relations for sediment transport quantities, based on steady uniform flows, can often provide poor comparisons with experiment data (Sumer *et al.*, 2003). Thus, the effect of turbulent fluctuations is of significant importance, particularly on how the sediment interacts with it.

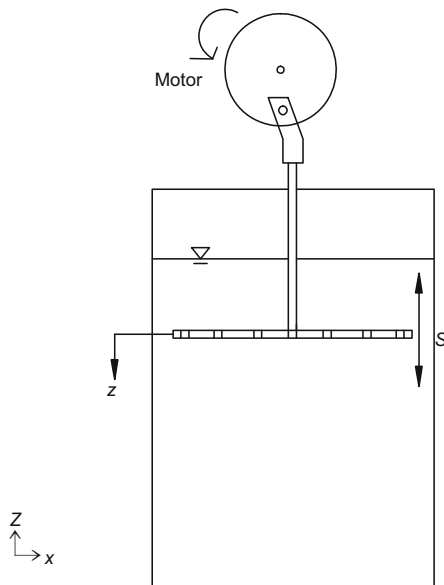


**Fig. 1** A typical oscillating-grid experimental setup. The grid is oscillated at fixed stroke length  $S$  and the distance away from the grid  $z$  starts at the mid-plane of the grid

The study of isolated turbulent fluctuations on sediment dates back to 1939 when Rouse (1939) studied the sediment suspension using turbulence generated from a vertically oscillating grid in a water tank. A typical oscillating-grid setup is shown in Fig. 1, where a motor continuously rotates a spindle and the planar grid is oscillated with a fixed distance (i.e., stroke length  $S$ ). In a laboratory frame, the

flow at sufficiently large distances from the grid ( $z$ ) is statistically stationary and the turbulence statistics of the tangential velocity components  $u$  and  $v$  only vary in the direction perpendicular to the grid plane  $z$  (Hopfinger and Toly, 1976; Wan Mohtar, 2016). Using this frame of reference, the grid turbulence can be modeled as statistically homogeneous and isotropic flow, which allows relatively complete statistical information to be provided by fewer measurements than that required for the classical shear flows. However, the undesired secondary flow (or circulation) is rather impossible to be completely eliminated and is treated as an intrinsic feature in the oscillating-grid turbulence (McKenna and McGillis, 2004). Even so, the inherent secondary circulation, of which the maximum length scale can be the size of the tank, may be eliminated through several rules of thumb in oscillating-grid turbulence experiments namely: (1) the frequency of oscillation is below 7 Hz (McDougall, 1979) or 8 Hz (Shy *et al.*, 1997); (2) the grid solidity is less than 0.4 (Mohamed and Larue, 1990); (3) the grid end condition ensures that the wall behaves as a plane of symmetry (whereby the distance between the last grid and the wall is made as small as possible) (Fernando and De Silva, 1993). It was suggested that the distance should be 3–4 mm (Voropayev *et al.*, 1995).

When these conditions are satisfied, the grid generated flow can be said to have an approximation of zero mean fluid velocities, thereby allowing the effect of turbulent fluctuations to be considered in isolation. The flow generated is a quasi-isotropic, laterally homogeneous turbulence and at distances further away from the grid, the decay of (time-averaged) root mean square (RMS) tangential velocity components ( $u, v$ ) and vertical velocity ( $w$ ) with depth below the grid's mid position  $z$  can be expressed as

$$u = v = C_1 f S^{3/2} M^{1/2} z^{-1}, \quad (1a)$$

$$w = C_2 f S^{3/2} M^{1/2} z^{-1}, \quad (1b)$$

where  $f$  is the oscillation frequency,  $M$  is mesh size, and the dimensionless constants  $C_1 = 0.25$  and  $C_2 = 0.27$  (Hopfinger and Toly, 1976; Cheng and Law, 2007). Eq. (1) is (only) applicable at  $z \gtrsim 2M$ , a region considered to reach the state of quasi-isotropic homogeneous turbulence (Hopfinger and Toly, 1976; Wan Mohtar, 2011). At this region, the isotropy ( $w/u = 1$ ) behavior is not always the case, where for higher stroke length anisotropy is highly likely

(Wan Mohtar, 2016). Even so,  $w/u$  is found to be around 1.5 (at  $S/M = 2$ ) and the generated flow can be considered as quasi-isotropic homogeneous turbulence. However, it should be noted that most of the studies discussed here employed relative stroke length  $S/M < 2$ . Therefore, the influence of anisotropy is trivial.

Several studies have employed oscillating-grid turbulence to investigate the threshold criteria for sediment movement (Bellinsky *et al.*, 2005; Wan Mohtar and Munro, 2013), sediment resuspension (Noh and Fernando, 1991; Huppert *et al.*, 1993; 1995; Michallet and Mory, 2004), and contaminant release from contaminated sediment (Valsaraj *et al.*, 1997; Cantwell *et al.*, 2008).

The turbulence intensity  $u/U$  (where  $U$  is the mean horizontal velocity) is high in the region near to the grid turbulence, particularly at  $z/M = 1$  due to the strong vertical direction of jet flow (from the grid oscillation motion) (Wan Mohtar, 2011). However, the intense interaction between the jet and wakes breaks down further away from the grid, where at distance  $z/M > 2$ , the large scale motions in the bulk flow are negligible and a quasi-isotropic homogeneous turbulence exists at that region (Hopfinger and Toly, 1976; Fernando and De Silva, 1993; Wan Mohtar, 2016). Most of the studies in incipient sediment motion were done with the bed surface at distance  $z/M > 2$  and the turbulence was produced following the rules of thumb discussed above.

The experimental setup of oscillating-grid turbulence has permitted in-depth investigations and provides a better understanding on how the turbulent fluctuations affect the sediment dynamics. This paper provides an account of how the grid-generated turbulence was used to investigate the incipient sediment motion and sediment suspension. The discussion includes the difference in analysis, common findings, and how the results were interpreted to explain the sediment transport.

## 2 Incipient sediment motion

Incipient sediment motion is the condition when a stationary grain receives fluid forces exceeding its friction force and submerged weight and eventually moves from its original position. The parameter used to describe the phenomenon is expressed as the critical Shields parameter  $\theta_c$ , where the concept was first

formulated by Shields (1936) using dynamic similarity between the critical bottom shear stresses  $\tau_c$  and the immersed weight of the grains. The term critical was used to denote the threshold criteria for sediment motion. The parameter  $\theta_c$  is defined as

$$\theta_c = \frac{\tau_c}{(\rho_s - \rho)gd}, \quad (2)$$

where  $\tau_c = \rho u_{*c}^2$  is the critical bed shear stress,  $u_{*c}$  is the critical shear velocity, i.e., a characteristic velocity defined at the near-bed region,  $g$  is the gravitational acceleration,  $d$  is the mean grain diameter, and  $\rho_s$  and  $\rho$  are the sediment and fluid densities, respectively.

The use of  $\tau_c$  as the critical parameter arises from the fact that in steady uniform flows, the statistics of the near-bed turbulence that induce sediment motion are scaled with the shear velocity  $u_{*c}$ . In an oscillating-grid experiment, where it is not possible to measure  $\tau_c$  directly, it is often expected that the critical bed shear stress will scale as  $\tau_c \sim \rho u_c^2$ , where  $u_c$  is often taken as the critical RMS horizontal velocity when the incipient sediment motion is observed.

The approximation of shear stress can be described as the turbulent kinetic energy  $k = \frac{1}{2}(u^2 + v^2 + w^2)$ , where the values of  $u$ ,  $v$ , and  $w$  were taken either at the distance close to the bed or at the bed itself. Assuming isotropy ( $u \approx v \approx w$ ), and using the RMS horizontal velocity  $u$  as described in Eq. (1), the critical Shields parameter (using oscillating-grid turbulence) is defined as

$$\theta_c = \frac{1.5C_1^2 f^2 S^3 M}{z_c^2 g(s-1)d}, \quad (3)$$

where  $z_c$  is the distance from the grid mid-plane to the point where  $u_c$  was taken, and  $s$  is the relative density define as  $\rho_s/\rho$ . As  $\theta_c \propto z_c^{-2}$ , the most important question posed was how the critical distance  $z = z_c$  value was determined. The most optimum point is at the near-bed region where the fluid forces directly act on the particles. However, the definition of points to be taken is subjective and may vary from study to study. For the characterization of  $\theta_c$  using turbulence generated by an oscillating grid, the studies of Lyn (1995), Medina (2002), Bellinsky *et al.* (2005), Liu *et al.* (2006), and Wan Mohtar and Munro (2013) were compared. As shown in Table 1, the  $z_c$  points chosen were not consistent between

studies and this will be further discussed. Not to be confused with the critical distance from the grid mid-plane  $z_c$ , the distance from the bed  $\mathcal{Z}$  will be used. For easier analysis, the dimensional distance  $\mathcal{Z}$  was made dimensionless by dividing by the sediment particle size for each study. Note that  $\mathcal{Z} = 0$  is the position of the top of the sediment bed. The corresponding non-dimensional distance  $\xi/\ell$ , that is made by dividing the distance  $\xi$  with the turbulent integral length scale  $\ell$ , is also shown in Table 1. Parameter  $\xi/\ell$  shows a wide range between 0.01–5.29 for the studies discussed here. As the entrainment of sediment is influenced by the fluid forces acting on it, it is anticipated that the relative distance of measurement point based on the sediment size gives a more appropriate criterion, and so the following discussion is based on this criterion.

The discussion starts with the work of Bellinsky *et al.* (2005), where their  $u_c$  measurement was taken at  $\mathcal{Z} \approx 5.08$  cm from the sediment bed. It is considered that at this distance, i.e.,  $25d \leq \mathcal{Z} \leq 668d$ , the fluid forces obtained are deemed not to be an accurate representation of the actual forces acting on the particles. Therefore, the  $\theta_c$  calculated using Eq. (3) at this point is expected to be misconstrued.

Liu *et al.* (2006) only employed one sediment particle size, that is  $d = 450 \mu\text{m}$ . The critical Shields parameter was obtained with the  $u_c$  value measured at  $0.5d$  (i.e., equivalent to  $0.025$  mm) above the bed surface. Although obtaining  $u_c$  at such distance is ideal, the dimensional distance gives inconsistent representation should a wide range of sediment sizes be used. For example, if the smallest sediment size (available) is  $80 \mu\text{m}$ , the equivalent  $\mathcal{Z}$  is at  $0.5d \approx 0.04$  mm, which is very small, and fluid velocity measurement techniques for measuring at such small distances are quite impractical.

Lyn (1995) and Medina (2002), in their experiments, employed the  $u_c$  values (calculated using Eq. (3)) at  $\mathcal{Z} = 1\text{--}5$  mm and  $\mathcal{Z} \approx d$  (i.e., the size of sediment examined) above the bed surface, respectively. In line with the previous discussion, for different sediment particle sizes,  $u_c$  will be taken at different (inconsistent) non-dimensional distances. At the near-bed region, the (quasi-isotropic homogeneous) turbulence characteristics change along the vertical distance from the bed. The presence of bed induces inhomogeneity within the near-bed region, where at this region (usually  $\mathcal{Z} \approx 1.5\ell$ ), Eq. (1) is

no longer valid. The  $u, v$  values are amplified and  $w$  is monotonically decreased due to the kinematic boundary condition (Perot and Moin, 1995; Bodart *et al.*, 2010). The significant changes to the turbulence structure in the near-bed region need to be accounted for and have a notable impact on the value of  $u_c$ , which (when calculated using Eq. (3)) underestimates the actual behavior (Wan Mohtar and Munro, 2013).

Wan Mohtar and Munro (2013) took a more rigorous analytical approach by considering how the presence of bedform affected the statistical properties of the turbulence in the near-bed region. Thus, taking into account the changes of turbulence structure at the near-bed region,  $u_c$  is measured as the amplified  $u$  (typically at  $\mathcal{Z}/\ell = 0.3$ ) for different sediment particle sizes and  $u_c$  will be taken at different (inconsistent) non-dimensional distances. This approach is more consistent and independent of the sediment size. Note that for the range of sediment sizes used here, the distance above the bed is  $4.5d \leq \mathcal{Z} \leq 62.5d$ , much lower than those observed in Bellinsky *et al.* (2005)'s experiments. Fig. 2 shows the  $\theta_c$  against the dimensionless particle Reynolds number  $\text{Re}_p = \sqrt{(s-1)gd^3}/\nu$  ( $\nu$  is the water kinematic viscosity) for data extracted from the studies shown in Table 1. It is obvious from the plot that the values of  $\theta_c$  vary according to where the measured  $u_c$  was taken, where Bellinsky *et al.* (2005)'s data shows a considerable lower value than measured using amplification RMS horizontal fluid velocity. This is expected as the amplified  $u$  may give an increment up to 20% greater than those calculated using Eq. (1) (Hunt and Graham, 1978).

For qualitative comparison with the standard profile obtained in steady turbulent channel flows, the values of  $\theta_c$  obtained were compared with the standard Shields curve (shown in Fig. 2 as a solid line), proposed by Brownlie (1982) as

$$\theta_c = 0.22\text{Re}_p^{-0.6} + 0.06 \exp(-17.77\text{Re}_p^{-0.6}). \quad (4)$$

Eq. (4) was developed in unidirectional, shear flows, where the mean flow is dominant and the flow behavior differs from grid-generated turbulent flow. As the turbulence level scales on the shear  $u_{\text{rms}} \sim \partial U/\partial y$ , where  $u_{\text{rms}}$  is an approximation of turbulence strength and shear velocity  $u_*$ . Recall that for the critical bed shear stress (where in shear flows,  $u_{*c}$  was used), the scaling  $\tau_c \sim \rho u_c^2$  in grid

**Table 1** Summary of selected incipient sediment motion research using an oscillating grid (Recall that  $z$  denotes the distance from the grid mid-plane to the sediment bed. The symbol  $\xi$  defines the distance above the bed surface where  $u_c$  is taken for the determination of the critical Shields parameter. Thus,  $z_c = z - \xi$ . The symbol  $Re_M$  denotes the Reynolds number, obtained as  $fSM/\nu$ . The Bellinsky point was obtained through private communication)

Study	$S/M$ (cm)	$Re_M$	$z$ (cm)	$\xi$	$\xi/\ell$	Range of $d$ ( $\mu\text{m}$ )	$s$
Lyn (1995)	1.0	$\approx 7200$	15	$\approx d$	0.01	150–180	2.46
Medina (2002)	1.5	350–600	2.95	1–5 mm	1.69	71–149	2.30
Liu <i>et al.</i> (2006)	0.6	1000–9000	13–20	$0.5d_{50}$	0.02	450	1.16
Bellinsky <i>et al.</i> (2005)	1.2	2187–4174	9.60	5.08 cm	5.29	76–2000	2.3–3.84
Wan Mohtar and Munro (2013)	1.6	2800–12400	16, 18	$\approx 0.1M$	0.31	80–1100	1.18 & 2.5

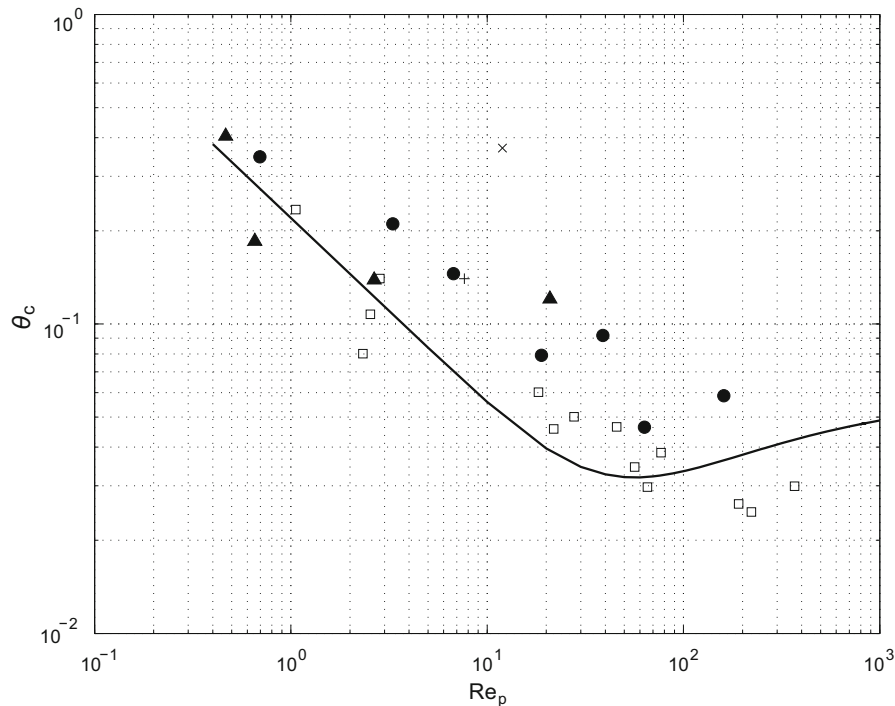


**Fig. 2** Measured critical Shields parameter  $\theta_c$  with data extracted from Lyn (1995) (+), Bellinsky *et al.* (2005) ( $\square$ ), and Liu *et al.* (2006) ( $\times$ ). Different sediment types from Wan Mohtar (2011) were represented as ballotini ( $\bullet$ ) and Diakon ( $\blacktriangle$ ). The solid line is the Shields curve calculated using the relationship from Brownlie (1982)

experiments permits both quantitative and qualitative comparisons with the standard Shields curve.

Note that for the hydraulically rough region (i.e.,  $Re_p \gtrsim 500$ ),  $\theta_c$  reached a constant value of around 0.06, whereas for the hydraulically smooth region ( $Re_p \lesssim 20$ ),  $\theta_c$  increases steadily with decreasing  $Re_p$ . The region between the two cases (i.e.,  $20 < Re_p < 500$ ) is commonly addressed as the transition region. Threshold criteria obtained using grid turbulence experiments show a qualitative similarity with the trend predicted by the standard Shields curve for the hydraulically smooth and transition regions. Although the turbulence charac-

teristics differ from those observed in the open channel flows, data shows a consistent trend with the curve obtained from channel-flow studies. It is interesting to see that although the employed  $u_c$  was considered invalid (due to its significant larger distance from the bed), the Bellinsky data shows the best agreement with the Shields curve. The data follows closely for the hydraulically smooth and lower transition regions, although were underestimated for  $Re_p > 100$ .

The similar Shields profile obtained indicates that the (well established) Shields diagram is an accurate representation for incipient sediment motion.

The grid-generated turbulence has a dominant horizontal velocity component ( $u$ ) and moves the sediment in the same manner as the averaged velocity in unidirectional flows.

Based on the analysis done, it was found that regardless of the position taken for critical velocity or how the incipient sediment motion was interpreted, the final outcome is that the Shields profile (obtained from near-bed turbulence) followed the original Shields curve (based on the unidirectional flow). This indicates that velocity fluctuations and turbulence play a similar role to the mean velocity, owing to the fact that the horizontal components (of the vortices) initiated the sediment movement. It directly implies that the established Shields curve still applies and is useful to predict the incipient sediment motion behavior.

### 3 Sediment resuspension

Resuspension is the event where the settled sediment is being entrained back (in this case by water) and redistributed back into the overlying column of water to an elevated height from the bed and be in suspension mode (for quite some time).

In investigating the sediment resuspension in an oscillating-grid experimental setup, the grid was placed near the bottom of the tank and vertically oscillated to generate quasi-isotropic homogeneous turbulence, as shown in Fig. 3, to emulate the turbulence conditions at the boundary layer. This configuration differs from the experiments conducted to obtain the incipient sediment motion where the grid was put further away from the sediment bed (typical setup is as shown in Fig. 1). Even so, it should be highlighted that most of the analysis on the turbulence on suspension was done at distances further away from the grid (and not at near-bed region), usually at  $z/M > 1.5$  in accordance with the standard grid turbulence vertical profile. As such, it can be said that the effect of secondary flow is rather negligible and the effect of turbulence on sediment suspension can be explicitly discussed.

Layers of particles were placed at the bottom of the tank to imitate a sediment bed and when the fluctuating forces significantly exceed both the critical Shields parameter  $\theta \gg \theta_c$  and the particle settling velocity  $\omega_T$ , the sediment is resuspended into the outer turbulent boundary layer. As the grid is

vertically oscillated, it is natural that the mean vertical velocity component is higher than the horizontal components, and this helps the sediment to be in suspension. If the flow is such that  $\theta \gg \theta_c$ , the sediments are continuously being entrained from the bed.

The sediment dispersion process (by the turbulence) from the bed is governed by the non-dimensional Rouse number  $Rou$  (ratio of the particle settling velocity  $\omega_T$  and the RMS vertical velocity  $w$ ) and Richardson number  $Ri$ , here expressed, respectively, as

$$Rou = \omega_T/w, \quad (5)$$

$$Ri = \frac{g'\ell C}{w^2}, \quad (6)$$

where  $g'$  denotes the reduced acceleration due to gravity,  $g' = g(\rho_s - \rho)/\rho$ , and  $C$  is the particle concentration within the suspension layer. The parameter  $Rou$  is often used to dictate the mode of sediment transport in a steady mean flow (characterized by the shear velocity  $u_*$  instead of  $w$  described here) whether the sediment moved as bedload (for  $Rou > 2.5$ ) or suspension (for  $Rou < 1.2$ ). For simplicity, the particle settling velocity  $\omega_T$  described in Eq. (5) is expressed as

$$\omega_T = \frac{4g(\rho - \rho_s)d^2}{3C_D\rho}, \text{ for } Re_p > 500, \quad (7)$$

where symbol  $C_D$  denotes drag coefficient. Note that the particle settling velocity discussed is based on a spherical particle in a turbulent regime flow, which is usually the case for sediment resuspension. This parameter is of paramount importance where the settling velocity may varied in suspension particularly for the settling clouds of differently shaped grains. However, most of the oscillating-grid turbulence studies omit the complexity of shape factor and mixed sediment sizes and focused on homogeneous spherical particles instead.

When the sediment is in suspension, the particles are subjected to the upward convection flux and the sedimentation downward flux. Eq. (6) describes the ratio of these fluxes presented as the (dimensionless) Richardson number  $Ri$ .

In the oscillating-grid experiments context, the upward flux is due to the turbulence intensity, which directly depends on the grid oscillation parameters (i.e., frequency  $f$ , stroke length  $S$ , and mesh  $M$ ).

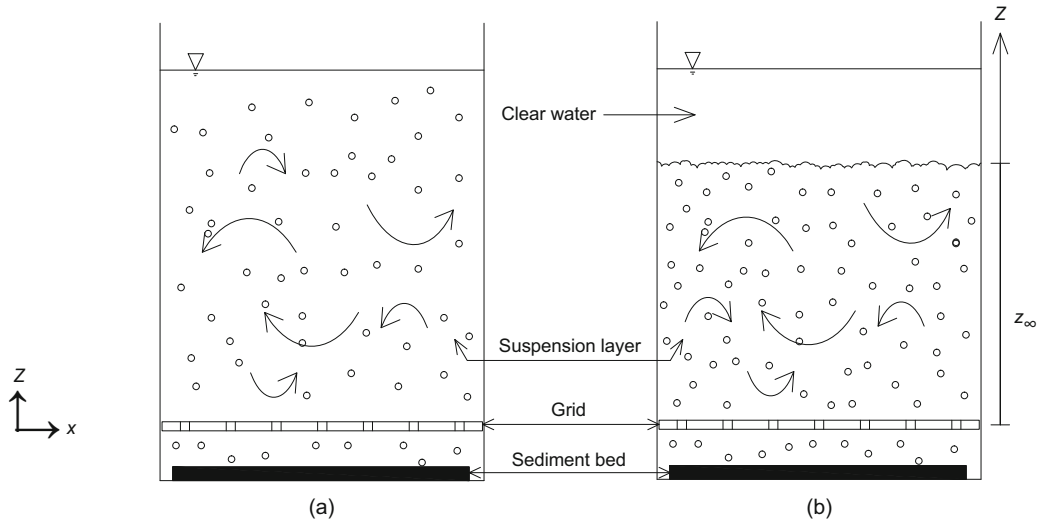


**Fig. 3** A typical oscillating-grid experimental setup for sediment resuspension, where the grid is placed at the bottom of the tank (Plots show suspension layer without lutocline (a) and with the formation of lutocline (b). Circular arrows and dots represent turbulence and concentration of suspended particles, respectively)

The downward flux on the other hand, is contributed by the particle concentrations and directly the particle settling velocity  $\omega_T$ .

Finer sediment particles are more easily entrained compared to coarser particles, which is obvious as inertial force due to submerged weight is less (Redondo *et al.*, 2001; Buscombe and Conley, 2012). The minimum velocity for sediment lift-off into the water column is a function of sediment size, and consolidation and resting times, where higher turbulence intensity is required as the mean sediment size  $d$  and consolidation time increase (Medina *et al.*, 2001). Non-consolidated or disturbed sediment may only require 63%–87% lower velocity values than what was needed for consolidated particles.

The sediment mass flux  $\phi$  within the suspension layer can be determined through the equilibrium of energy balance between the total kinetic energy (from the grid), potential energy of the dense layer, and the turbulence dissipation (Sanchez and Redondo, 1998). The parameter  $\phi$  is expressed as

$$\phi = h \frac{d}{dt} \bar{C}, \quad (8)$$

where  $h$  is the water depth, and  $\bar{C}$  is the averaged concentration in a column (Sanchez and Redondo, 1998; Redondo *et al.*, 2001). The concentration profile commonly follows the power-law profile, that is high sediment concentration is observed at near-bed region, and the concentration diminishes at distances

further away from the bed.

Continuous particle resuspension results in increasing particle concentration  $C$  (above the bed), and a suspension layer is established. As previously discussed, the concentration of particles is determined based on the sediment mass balance, that is the net outcome of the lift forces (sediment diffusivity  $\epsilon_s$ ) and the settling velocity of the grain particles. Sediment diffusivity  $\epsilon_s$  is expressed in terms of turbulent momentum diffusivity, often described using the turbulent eddy viscosity  $\nu_t$ . The ratio of turbulent eddy viscosity  $\nu_t$  to  $\epsilon_s$ , known as Schmidt number  $Sc$ , is presented as

$$Sc = \frac{\nu_t}{\epsilon_s}. \quad (9)$$

The parameter  $\epsilon_s$  can be described as constant, linear, and parabolic which gives exponential suspended sediment concentration profiles and power law for both linear and parabolic types of sediment diffusivity.

In sheared open channel flow,  $Sc \approx 1$ , which is considered as the simplest approach (Chanson, 2004). However,  $Sc$  may have a value greater than 1 when the particle settles down through turbulent eddies (Fredsoe *et al.*, 1985) and  $Sc < 1$  when the centrifugal forces exert larger effect on particles than they do on the neighboring fluid (Davies and Thorne, 2005).

Grid turbulence experiments showed that Schmidt number is dependent on grain size and

turbulence intensity, and  $Sc$  value is often greater than 1. Bigger  $Sc$  was found for smaller sediment size and higher turbulent flow (Nielsen and Teakle, 2004; Buscombe and Conley, 2012). Consequently,  $\epsilon_s$  for fine sediment has lower values than coarse sediment, which may be due to the diminishing gradient as more sediment is entrained and kept in suspension, increasing the concentration of suspended sediment (Amoudry *et al.*, 2005).

### 3.1 Formation of lutocline

The layer (of sediment entrained) may be continuously deepened until it reaches a steady-state suspension layer with a depth of  $z_\infty$ . However, the layer depth and the particle concentration can vary since the particles may be kept in suspension or settled. It has been found that for flows  $\theta \gg \theta_c$ , three modes of particle suspension can be achieved depending on the turbulence intensity  $I = w/W$ , where  $W$  denotes the mean vertical velocity (Huppert *et al.*, 1995). The suspension modes are: (1) where all particles are settled; (2) particles within the layer are simultaneously in suspension and settled; (3) where all particles are kept in suspension. Depending on the particle size, each mode of suspension has its own critical intensity. For example, for flows with turbulence intensity  $I_1 < I < I_3$ , where the subscripts 1 and 3 denote the modes of suspension, respectively, the suspension mode 2 should be observed, that is, some of the particles fall to the bottom while others remain in the suspension layer.

The (final) steady-state suspension depth can be obtained using the empirical equation, described as

$$z_\infty = f\ell^2 \left( \frac{g'w_T C_\infty}{A\rho_s} \right)^{-1/3}, \quad (10)$$

where  $C_\infty$  denotes the steady-state concentration,  $\ell = 0.1z$  is the turbulent integral length scale, and  $A$  is an empirical value, often taken as 3.6 (Noh and Fernando, 1991; Zhou and Cheng, 2008).

Theoretically, the turbulence intensity  $I$  also indirectly defines the thickness of the steady-state suspension layer, where  $z_\infty$  increases as the turbulence intensity increases. However, at a certain limit of high intensity, the particles in suspension have a significant impact on the turbulence characteristics (Michallet and Mory, 2004). For flows with smaller  $Rou < 0.01$  (that is high turbulence intensity), the increased concentration of the particles within the

suspension layer suppresses the upward turbulence, reducing the eddy diffusivity. The local reduction of the diffusion introduces a strong concentration gradient at a certain depth, where the turbulence is suppressed even more, inhibiting both the diffusion of particles and the propagation of turbulent energy so that the particles are closely clustered (Noh and Fernando, 1991). This depth, known as lutocline (in oceanographic terminology), is the interface separating the heavy sediment-laden bottom layer and the clear water top layer, as shown in Fig. 3b.

Noh and Fernando (1991), in their numerical modeling, established the existence of a lutocline based on the (critical) Richardson value  $Ri_c \approx 2.2Rou^2$ . When lutocline appears (for flows with  $Ri > Ri_c$ ), the concentration of particles is almost uniform within the suspension layer. The effect from inertial forces is insignificant within the vicinity of the lutocline, where using mean averaged flow velocity, smaller  $Ri < 0.25$  values were obtained (Ivey and Imberger, 1991). However, grid-generated turbulence experiments showed  $Ri \approx 1$  at near-lutocline, indicating that the turbulence is energetic and sufficient to keep the particles in suspension (Michallet and Mory, 2004).

Where there is a lutocline, the concentration of particles,  $-dC/dz$ , increases with  $z$  before rapidly decreases to zero at the formation of horizontal front (or lutocline) (Noh and Fernando, 1991). At the lutocline surface (i.e.,  $d^2C/dz^2 = 0$ ), the turbulent kinetic energy rapidly decreases (due to turbulence decay) and the vorticity remains constant, independent of the turbulence intensity (Noh and Fernando, 1991; Medina *et al.*, 2001).

For flows below the critical Richardson value  $Ri_c$ , no lutocline is formed. There is no sharp concentration gradient, as shown in Fig. 3a, and the particle concentration monotonically decreases with increasing distance from the grid (Noh and Fernando, 1991). At such flow, the decreasing particle concentration limits the buoyancy effect and the inertial forces keep the particle in suspension, subsequently increasing the suspension layer  $z_\infty$  (Huppert *et al.*, 1995).

Using Eq. (10), the height of lutocline occurrence may be predicted. Consequently, the height of concentrated benthic suspension or 'fluid mud' may be accurately determined. Fluid mud is also the term used to describe the high concentration layer of



suspended fine sediment (with sizes  $< 63 \mu\text{m}$ ) which is often in the range from 10 to  $300 \text{ kg/m}^3$ . Fine-grained cohesive sediment, consisting mainly of silt and clay is entrained as suspended load and mostly occurs in estuarine maximum zones (ETMZs) (Liu *et al.*, 2006). The occurrence of fluid mud might restrain navigability and fine sediment is known to often be a carrier of pollutants as the sediment specifically absorbs contaminants available in the overlying water. Even so, it should be noted that the water depth should be considered, where when  $z_\infty > h$ , the lutoclines do not appear (in estuaries) (Wolanski *et al.*, 1998).

### 3.2 Effect on the settling velocity

Previously it has been discussed that the thickness of the (steady-state) suspension layer  $z_\infty$  depends on the turbulence intensity, but the settling characteristics also play an important role. The particle settling velocity value calculated using Eq. (7) was developed based on a turbulent regime flow. However, the presence of turbulence modifies the settling velocity by either enhancement or retardation, so that the particle settling velocity deviates significantly from the still water terminal velocity  $\omega_T$ . The reduction of the particle settling velocity is due to the nonlinear drag and loitering effect (Nielsen, 1992; Mei, 1994; Zhou and Cheng, 2008). On the other hand, the enhancement of settling velocity is attributed to the preferential sweeping or (downward) trajectory bias of a (coherent) turbulence structure (Wang and Maxey, 1993). Thus, the particles are not settled at a constant rate of gravity, but instead are fluctuated and dependent on the turbulence structure within the flow.

The turbulence-modified particle settling velocity  $\omega_s$  depends on the mean vertical fluid velocity component  $W$  and fluctuating vertical velocities  $w$ . When  $W$  is dominantly in the downward direction,  $\omega_s$  is enhanced and adverse effect of  $\omega_s$  is observed when  $W$  is upward. The turbulence-induced reduction in settling velocity is due to the indefinite location of flow separation around the particle which affects the vortex shedding characteristics and drag.

Although the turbulence-particle interaction effect limits the ability to exactly predict the turbulence-modified settling velocity  $\omega_s$ , it can be estimated (reasonably well) as

$$|\omega_s| = \frac{|\omega_T|}{1 + \frac{W}{\omega_T} + W^2 + \frac{w^2}{|\omega_T^2|}}, \quad (11)$$

given by Zhou and Cheng (2008). From this, it can be seen that the  $\omega_s$  is clearly influenced by both mean vertical velocity and turbulence intensity.

The dynamic interaction of particles with coherent eddy structures is much stronger than with a random flow field and possibly lasts a longer period of time (Zhou and Cheng, 2008). It was shown in open channel studies, that near the bottom, the coherent streamwise vortices (also known as funnel vortex) can maintain heavier particles in suspension through ejection and accelerate the settling velocity through sweep motion. An increment up to 10%–25% of settling velocity was found, assisted by the fluid motions in the flow (Noguchi and Nezu, 2009). Supported by the findings from open channel experiments, the effect of isolated turbulence on the settling velocity was conducted where the turbulence-modified particle settling velocity  $\omega_s$  has been found to vary within the range of  $0.25\omega_T \leq \omega_s \leq 1.6\omega_T$  (Nielsen, 1992; Zhou and Cheng, 2008). The effect from turbulence is seen to be crucial and supports the findings from open channel studies.

The turbulence-modified particle settling velocity  $\omega_s$  initially was thought to be a function of the Stokes number, a dimensionless parameter characterizing the particle behavior in suspension. It reflects the time taken for a particle to respond to an interacting turbulent eddy, expressed as

$$\text{St} = \frac{\tau_p}{T_L}, \quad (12)$$

where  $\tau_p = \omega_T/g$  denotes the particle relaxation time.  $T_L$  is the turbulent time scale, and can be taken as the integral time scale  $T_L = u/\ell$ , or the Kolmogorov scale  $T_L = \tau_\eta = u/\epsilon$ , where  $\epsilon$  denotes the dissipation rate (Aliseda *et al.*, 2002). The maximum effect of the turbulence-induced particle settling velocity that is either reduction or enhancement is best observed at  $\text{St} \approx 1$ , that is, when the particle motion has the same velocity as the turbulent motion (Yang and Shy, 2005; Doroodchi *et al.*, 2008). However, there was no distinctive trend observed for the suspended sediment behavior with Stokes number.

The increasing of  $\omega_s$  was also found to depend on the particle loading, where  $\omega_s$  increases as the volume fraction of particles in the flow increases and

is considered valid for the entire range of  $St$  (Aliseda *et al.*, 2002).

The presence of turbulence accumulates heavier particles in regions of high strain rate and low vorticity, leading to an inhomogeneous, intermittent concentration field, and induces the creation of clusters of particles (Aliseda *et al.*, 2002; Zhou and Cheng, 2008). These accumulated particles, which usually occur at the bed, are obviously denser and increase in numbers as the volume fraction of particles in the flow increases. As these clusters settle, they interact with other particles by entraining them and subsequently increasing their relative density and accelerating their settling velocity. At a higher Stokes number, where the particle diameter is much larger than the turbulence scale, the available turbulence eddies are too small to carry the particle along its path (Orlins and Gulliver, 2003). The larger particle which has a longer relaxation time is not entrained but instead is pushed aside and agglomerated on the bed. Smaller particle, on the other hand, with low inertia and short relaxation time, closely follows the fluid motion and is suspended even further away from the bed (Kaftori *et al.*, 1995).

The changes in the value of settling velocity obviously affect the Rou number and the determination of the type of sediment movement. For flow with high turbulence, using Eq. (7) might not be the best way forward to interpret the sediment behavior. The grid turbulence experiments discussed show that particle settling velocity is affected by the particle concentration, sediment characteristics, and coherent vortex structures, and the determination of settling velocity is complicated by the inter-relation between these parameters.

### 3.3 Grid turbulence on other parameters

In the complexity of sediment-turbulence interaction within the suspension layer, lots of parameters may affect the suspension process but they have been often simplified in laboratory conditions. Other parameters include inhomogeneous particle size distribution, the effect of salinity, cohesive sediments, and consolidation effect. Each parameter will be discussed in the following paragraphs, starting with the inhomogeneity in particle sizes of the bed materials.

When the sediment bed varies in particle size distribution and is non-uniformly distributed, particle concentration gradient develops where fine sed-

iments are kept in suspension higher in the outer flow and bigger particles are at the near-bed region or settled at the bottom. As the particles settle to the bed via gravitational forces with a relationship of  $\omega_T \propto d^2$  (recall Eq. (7)), it is expected that bigger particles with faster settling velocity reside at the near-bed region. Thus, for a wide particle size distribution, the use of  $\omega_T$  of a representative sediment size may be inaccurate and the value  $\omega_T$  of each class of sediment size needs to be accounted for. The effect of non-uniformity of bed material has received considerable attention, where the sediment is often described as using an effective representative size considering the varying available sediment sizes, i.e., size gradation factor  $K_d$  (Molinas and Wu, 1998; Wu *et al.*, 2004). Considering the effective size might give a better representation of the settling velocity; hence, the suspension behavior and determination of suspension layer depth may differ, although this is yet to be proven.

Most of the studies discussed up to now were based on the experiments conducted using non-cohesive sediments (Huppert *et al.*, 1995; Orlins and Gulliver, 2003). However, in practice, for example, marine sediments, the particles usually fall under the category of cohesive sediment (with sizes  $d < 30 \mu\text{m}$ ). These kinds of sediment are particularly difficult to characterize in the laboratory as their particle settling velocity differs and varies with concentration (Michallet and Mory, 2004). Furthermore, the density difference in flow due to salinity, and the flocculation of cohesive riverine or marine colloids are greatly promoted. The agglomerated particles increase the particle size and this obviously may impose an effect on the settling characteristics and change the behavior of the mixing within the suspension layer (Jensen, 1997).

Another important parameter often overlooked is the consolidation of the sediment. It is expected that when the sediment is well consolidated, the entrainment or resuspension from the bed would require higher bed shear stress  $\theta \gg \theta_c$  (Medina, 2002). That is, a higher turbulence intensity is needed to initiate sediment movement than would be estimated using Eq. (4). However, such effect is only valid up to a certain critical value, where above the value, the consolidation period has minimal impact (Orlins and Gulliver, 2003).

## 4 Conclusions

Oscillating grid has proven to be a successful alternative tool and experimental procedure in expressing the effect of isolated turbulent fluctuations on the phenomenon of sediment transport, i.e., incipient sediment motion and sediment resuspension. The implementation of the RMS fluid velocity gives a consistent representation of the flow behavior, in particular at the near-bed region, where the turbulent fluctuations are dominant.

Despite a different interpretation of the critical RMS horizontal velocity to characterize the threshold criteria, the Shields profiles obtained using the oscillating-grid experiments are qualitatively similar to the established Shields diagram obtained from a uniform steady flow. This indicates that the turbulent fluctuations do play a significant role in the incipient sediment motion. For smaller particle sediments, that is within the hydraulically smooth region,  $\theta_c$  is monotonically increased as the sediment size gets smaller and almost reaches a constant value for a bigger sediment size.

The method of oscillating-grid turbulence has been found to be more rigorously done for the sediment resuspension including the investigation of the formation of lutocline, the turbulence-modified settling velocity, concentration profile within the suspension layer, and consolidation of sediment. The concentration profile within the suspension layer, which defines the formation of lutocline, is interrelated with the sediment characteristics and the turbulence structure. The particle settling velocity  $\omega_T$ , which directly contributes to the Richardson and Stokes numbers, is the crucial parameter and highly influenced by the sediment size distribution and fluid motions.

The investigation of the sole effect of turbulence on the incipient sediment motion and sediment resuspension provides not only qualitatively similar findings to open channel studies but also contributes to an in-depth explanation of the physical interaction of flow-sediment. These experiments offer a conceptual link and help engineers, sedimentologists, and researchers understand the effect of turbulent fluctuations on sediment dynamics.

On a new note, the method of oscillating-grid turbulence provides possibilities for exploration in other sediment-related studies, in terms of the influ-

ence of vortex dipoles (or quadrupoles), flow topology characteristics (where most of the studies employed flat bed), and sediment contaminated release during suspension. The effect of turbulence on sediment suspension (in particular), over varying bed-form such as ripple, dune, and antidune, is yet to be investigated in detail. For further information on the formation of dipolar vortex, the reader is referred to the work conducted by Voropayev *et al.* (1995) and Voropayev and Fernando (1996).

## References

- Aliseda, A., Cartellier, A., Hainaux, F., *et al.*, 2002. Effect of preferential concentration on the settling velocity of heavy particles in homogeneous isotropic turbulence. *Journal of Fluid Mechanics*, **468**:77-105.  
<http://dx.doi.org/10.1017/S0022112002001593>
- Amoudry, L., Hsu, T.J., Liu, P.L.F., 2005. Schmidt number and near-bed boundary condition effects on a two-phase dilute sediment transport model. *Journal of Geophysical Research*, **110**:C09003.  
<http://dx.doi.org/10.1029/2004JC002798>
- Bellinsky, M., Rubin, H., Agnon, Y., *et al.*, 2005. Characteristics of resuspension, settling and diffusion of particulate matter in a water column. *Environmental Fluid Mechanics*, **5**:415-441.  
<http://dx.doi.org/10.1007/s10652-004-7302-3>
- Bodart, J., Cazalbou, J., Joly, L., 2010. Direct numerical simulation of unsheared turbulence diffusing toward a free-slip or no-slip surface. *Journal of Turbulence*, **11**:1-17.  
<http://dx.doi.org/10.1080/14685248.2010.521632>
- Brownlie, W.R., 1982. Prediction of Flow Depth and Sediment Discharge in Open Channels. PhD Thesis, California Institute of Technology, Pasadena, USA.  
<http://dx.doi.org/10.7907/Z9KP803R>
- Buscombe, D., Conley, D., 2012. Schmidt number of sand suspensions under oscillating grid turbulence. *Coastal Engineering Proceedings*, **1**(33):20.  
<http://dx.doi.org/10.9753/icce.v33.sediment.20>
- Cantwell, M., Burgess, R., King, J., 2008. Resuspension of contaminated field and formulated reference sediments. Part I: evaluation of metal release under controlled laboratory conditions. *Chemosphere*, **73**:1824-1831.  
<http://dx.doi.org/10.1016/j.chemosphere.2008.08.007>
- Chanson, H., 2004. The Hydraulics of Open Channel Flow: an Introduction. Elsevier Butterworth-Heinemann.
- Cheng, N.S., Law, A.W.K., 2007. Measurements of turbulence generated by oscillating grid. *Journal of Hydraulic Engineering*, **127**:201-207.  
[http://dx.doi.org/10.1061/\(ASCE\)0733-9429\(2001\)127:3\(201\)](http://dx.doi.org/10.1061/(ASCE)0733-9429(2001)127:3(201))
- Davies, A.G., Thorne, P.D., 2005. Modelling and measurement of sediment transport by waves in the vortex ripple regime. *Journal of Geophysical Research*, **110**:C05017.  
<http://dx.doi.org/10.1029/2004JC002468>
- Doroodchi, E., Evans, G., Schwarz, M., *et al.*, 2008. Influence of turbulence intensity on particle drag coefficients. *Chemical Engineering Journal*, **135**:129-134.  
<http://dx.doi.org/10.1016/j.cej.2007.03.026>

- Fernando, H.J.S., de Silva, I.P.D., 1993. Note on secondary flows in oscillating-grid, mixing-box experiments. *Physics of Fluids*, **5**:1849-1851. <http://dx.doi.org/10.1063/1.858808>
- Fredsoe, J., Andersen, A.H., Silberg, S., 1985. Distribution of suspended sediment in large waves. *Journal of Waterway, Port, Coastal and Ocean Engineering*, **11**:1041-1059. [http://dx.doi.org/10.1061/\(ASCE\)0733-950X\(1985\)111%3A6\(1041\)](http://dx.doi.org/10.1061/(ASCE)0733-950X(1985)111%3A6(1041))
- Hopfinger, E.J., Toly, J.A., 1976. Spatially decaying turbulence and its relation to mixing across density interfaces. *Journal of Fluid Mechanics*, **78**:155-175. <http://dx.doi.org/10.1017/S0022112076002371>
- Hunt, J., Graham, J., 1978. Free-stream turbulence near plane boundaries. *Journal of Fluid Mechanics*, **84**:209-235. <http://dx.doi.org/10.1017/S0022112078000130>
- Huppert, H.E., Turner, J.S., Hallworth, M.A., 1993. Sedimentation and mixing of a turbulent fluid suspension: a laboratory study. *Journal of Fluid Mechanics*, **114**:259-267. [http://dx.doi.org/10.1016/0012-821X\(93\)90029-9](http://dx.doi.org/10.1016/0012-821X(93)90029-9)
- Huppert, H.E., Turner, J.S., Hallworth, M.A., 1995. Sedimentation and entrainment in dense layers of suspended particles stirred by an oscillating grid. *Journal of Fluid Mechanics*, **289**:263-293. <http://dx.doi.org/10.1017/S0022112095001339>
- Ivey, G., Imberger, J., 1991. On the nature of turbulence in a stratified fluid. Part I: the energetics of mixing. *Journal of Physical Oceanography*, **21**:650-658. [http://dx.doi.org/10.1175/1520-0485\(1991\)021<0650:OTNOTI>2.0.CO;2](http://dx.doi.org/10.1175/1520-0485(1991)021<0650:OTNOTI>2.0.CO;2)
- Jensen, A., 1997. Experiments and Modeling of Turbulence, Salinity and Sediment Concentration Interactions in a Simulated Estuarine Water Column. MS Thesis, Cornell University, New York, USA.
- Kaftori, D., Hetsroni, G., Banerjee, S., 1995. Particle behavior in the turbulent boundary layer. I. Motion, deposition and entrainment. *Physics of Fluids*, **7**:1095-1105. <http://dx.doi.org/10.1063/1.868551>
- Lamb, M.P., Dietrich, W.E., Venditti, J.G., 2008. Is the critical Shields stress for incipient sediment motion dependent on channel-bed slope? *Journal of Geophysical Research*, **113**:1-20. <http://dx.doi.org/10.1029/2007JF000831>
- Liu, C., Huhe, A., Tao, L., 2006. Sediment incipience in turbulence generated in a square tank by a vertically oscillating grid. *Journal of Coastal Research*, **39**:465-468.
- Lyn, D.A., 1995. Observations of initial sediment motion in a turbulent flow generated in a square tank by a vertically oscillating grid. ASCE Water Resources Engineering Conference, p.608-612.
- McDougall, T.J., 1979. Measurements of turbulence in a zero-mean-shear mixed layer. *Journal of Fluid Mechanics*, **94**:409-431. <http://dx.doi.org/10.1017/S0022112079001105>
- McKenna, S.P., McGillis, W.R., 2004. Observations of flow repeatability and secondary circulation in an oscillating grid-stirred tank. *Physics of Fluids*, **16**:3499-3502. <http://dx.doi.org/10.1063/1.1779671>
- Medina, P., 2002. Start of Sediment Motion and Re-suspension in Turbulent Flows: Applications of Zero-mean Flow Grid Stirred Turbulence on Sediment Studies. PhD Thesis, Universidad Politécnic de Cataluña, Barcelona, Spain.
- Medina, P., Sanchez, M.A., Redondo, J.M., 2001. Grid stirred turbulence: applications to the initiation of sediment motion and lift-off studies. *Physics and Chemistry of the Earth (B)*, **26**:299-304. [http://dx.doi.org/10.1016/S1464-1909\(01\)00010-7](http://dx.doi.org/10.1016/S1464-1909(01)00010-7)
- Mei, R., 1994. Effect of turbulence on the particle settling velocity in the nonlinear drag range. *International Journal of Multiphase Flow*, **20**:273-284. [http://dx.doi.org/10.1016/0301-9322\(94\)90082-5](http://dx.doi.org/10.1016/0301-9322(94)90082-5)
- Michallet, H., Mory, M., 2004. Modelling of sediment suspensions in oscillating grid turbulence. *Fluid Dynamics Research*, **35**:87-106. <http://dx.doi.org/10.1016/j.fluidyn.2004.04.004>
- Mohamed, M.S., Larue, J.C., 1990. The decay power law in grid-generated turbulence. *Journal of Fluid Mechanics*, **219**:195-214. <http://dx.doi.org/10.1017/S0022112090002919>
- Molinas, A., Wu, B.S., 1998. Effect of size gradation on transport of sediment mixtures. *Journal of Hydraulic Engineering*, **124**:786-793. [http://dx.doi.org/10.1061/\(ASCE\)0733-9429\(1998\)124:8\(786\)](http://dx.doi.org/10.1061/(ASCE)0733-9429(1998)124:8(786))
- Nelson, J., Shreve, R., McLean, S., et al., 1995. Role of near-bed turbulence structure in bed-load transport and bed form mechanics. *Water Resources Research*, **31**:2071-2086. <http://dx.doi.org/10.1029/95WR00976>
- Nielsen, P., 1992. Coastal Bottom Boundary Layers and Sediment Transport. World Scientific, Mainland Press, Singapore.
- Nielsen, P., Teakle, I.A.L., 2004. Turbulent diffusion of momentum and suspended particles: a finite-mixing-length-theory. *Physics of Fluids*, **16**:2342-2348. <http://dx.doi.org/10.1063/1.1738413>
- Niño, Y., Garcia, M.H., 1996. Experiments on particle-turbulence interactions in the near-wall region of an open channel flow: implications for sediment transport. *Journal of Fluid Mechanics*, **326**:285-319. <http://dx.doi.org/10.1017/S0022112096008324>
- Noguchi, K., Nezu, I., 2009. Particle-turbulence interaction and local particle concentration in sediment-laden open-channel flows. *Journal of Hydro-environment Research*, **3**:54-68. <http://dx.doi.org/10.1016/j.jher.2009.07.001>
- Noh, Y., Fernando, H., 1991. Dispersion of suspended particles in turbulent flow. *Physics of Fluids A*, **3**:1730-1740. <http://dx.doi.org/10.1063/1.857952>
- Orlins, J.J., Gulliver, J.S., 2003. Turbulence quantification and sediment resuspension in an oscillating grid chamber. *Experimental in Fluids*, **34**:662-677. <http://dx.doi.org/10.1007/s00348-003-0595-z>
- Parker, C., Clifford, N.J., Thorne, C.R., 2011. Understanding the influence of slope on the threshold of coarse grain motion: revisiting critical stream power. *Geomorphology*, **126**:61-65. <http://dx.doi.org/10.1016/j.geomorph.2010.10.027>

- Perot, B., Moin, P., 1995. Shear-free turbulent boundary layers. Part I. Physical insights into near-wall turbulence. *Journal of Fluid Mechanics*, **295**:199-227. <http://dx.doi.org/10.1017/S0022112095001935>
- Redondo, J.M., de Madron, X.D., Medina, P., *et al.*, 2001. Comparison of sediment resuspension measurements in sheared and zero-mean turbulent flows. *Continental Shelf Research*, **32**:2095-2103. [http://dx.doi.org/10.1016/S0278-4343\(01\)00044-9](http://dx.doi.org/10.1016/S0278-4343(01)00044-9)
- Rouse, H., 1939. Experiments on the mechanics of sediment suspension. Proceedings of the 5th International Congress of Applied Mechanics, p.550-554.
- Sanchez, M.A., Redondo, J.M., 1998. Observations from grid stirred turbulence. *Applied Scientific Research*, **59**:243-254. <http://dx.doi.org/10.1023/A:1001139623537>
- Shields, A., 1936. Application of Similarity Principles and Turbulence Research in Bed-load Movement. Soil Conservation Service Cooperative Library, California Institute of Technology, Pasadena, USA.
- Shvidchenko, A.B., Pender, G., 2000. Flume study of the effect of relative depth on the incipient motion of coarse uniform sediments. *Water Resources Research*, **36**:619-628. <http://dx.doi.org/10.1029/1999WR900312>
- Shy, S., Tang, C., Fann, S., 1997. A nearly isotropic turbulence generated by a pair of vibrating grids. *Experimental Thermal and Fluid Science*, **14**:251-262. [http://dx.doi.org/10.1016/S0894-1777\(96\)00111-2](http://dx.doi.org/10.1016/S0894-1777(96)00111-2)
- Srinivasan, V.S., Cavalcante, R.G., Santos, C.A.G., 2008. A comparative study of some of the sediment transport equations for an alluvial channel with dunes. *Journal of Urban and Environmental Engineering*, **2**:28-32. <http://dx.doi.org/10.4090/juee.2008.v2n1.028032>
- Sumer, B.M., Chua, L., Cheng, N., *et al.*, 2003. Influence of turbulence on bed load sediment transport. *Journal of Hydraulic Engineering*, **129**:585-596. [http://dx.doi.org/10.1061/\(ASCE\)0733-9429\(2003\)129%3A8\(585\)](http://dx.doi.org/10.1061/(ASCE)0733-9429(2003)129%3A8(585))
- Valsaraj, K., Ravikrishna, R., Orlins, J., *et al.*, 1997. Sediment-to-air mass transfer of semi-volatile contaminants due to sediment resuspension in water. *Advances in Environmental Research*, **1**:145-159.
- van Rijn, L.C., 2007. Unified view of sediment transport by currents and waves. II: suspended transport. *Journal of Hydraulic Engineering*, **133**(6):668-689. [http://dx.doi.org/10.1061/\(ASCE\)0733-9429\(2007\)133%3A6\(668\)](http://dx.doi.org/10.1061/(ASCE)0733-9429(2007)133%3A6(668))
- Voropayev, S.I., Fernando, H.J.S., 1996. Propagation of grid turbulence in homogeneous fluids. *Physics of Fluids*, **8**:2435-2440. <http://dx.doi.org/10.1063/1.869028>
- Voropayev, S.I., Afanasyev, Y.D., van Heijst, G.J.F., 1995. Two-dimensional flows with zero net momentum: evolution of vortex quadrupoles and oscillating grid turbulence. *Journal of Fluid Mechanics*, **282**:21-44. <http://dx.doi.org/10.1017/S0022112095000024>
- Wan Mohtar, W.H.M., 2011. The Interaction of Oscillating-grid Turbulence with a Sediment Layer. PhD Thesis, University of Nottingham, Nottingham, UK.
- Wan Mohtar, W.H.M., 2016. Oscillating-grid turbulence at large strokes: revisiting the equation of hopfinger and toly. *Journal of Hydrodynamics*, **28**:373-381. [http://dx.doi.org/10.1016/S1001-6058\(16\)60651-0](http://dx.doi.org/10.1016/S1001-6058(16)60651-0)
- Wan Mohtar, W.H.M., Munro, R.J., 2013. Threshold criteria for incipient sediment motion on an inclined bedform in the presence of oscillating-grid turbulence. *Physics of Fluids*, **25**:015103. <http://dx.doi.org/10.1063/1.4774341>
- Wang, L., Maxey, M., 1993. Settling velocity and concentration distribution of heavy particles in homogeneous isotropic turbulence. *Journal of Fluid Mechanics*, **256**:27-68. <http://dx.doi.org/10.1017/S0022112093002708>
- Wolanski, E., Chappell, J., Ridd, P., *et al.*, 1998. Fluidisation of mud in estuaries. *Journal of Geophysical Research*, **93**:2351-2361. <http://dx.doi.org/10.1029/JC093iC03p02351>
- Wu, B., Molinas, A., Julien, P.Y., 2004. Bed-material load computations for nonuniform sediments. *Journal of Hydraulic Engineering*, **130**:1002-1012. [http://dx.doi.org/10.1061/\(ASCE\)0733-9429\(2004\)130%3A10\(1002\)](http://dx.doi.org/10.1061/(ASCE)0733-9429(2004)130%3A10(1002))
- Yang, T., Shy, S., 2005. Two-way interaction between solid particles and homogeneous air turbulence: particle settling rate and turbulence modifications measurements. *Journal of Fluid Mechanics*, **526**:171-216. <http://dx.doi.org/10.1017/S0022112004002861>
- Zhou, Q., Cheng, N., 2008. Experimental investigation of single particle settling in turbulence generated by oscillating grid. *Chemical Engineering Journal*, **149**:289-300. <http://dx.doi.org/10.1016/j.cej.2008.11.004>

## 中文概要

**题目:** 通过振荡网格实验研究初始泥沙运动和沉积物再悬浮

**概要:** 本文系统地研究了振荡网格生成的湍流效应对初始泥沙运动和沉积物再悬浮的影响,总结了影响泥沙运动和沉积的因素,给出了沉积物在宏观角度移动的基本概念和观点,并详细讨论了湍流对于沉降速度的影响。结果表明,湍流扰动对初始泥沙运动有重要影响。悬浮层内的浓度分布与沉积物特征和湍流结构有关。粒子沉降速度是一个关键参数,它主要受泥沙粒径分布和流体运动影响。

**关键词:** 振荡网格湍流; 初始泥沙运动; 沉积物再悬浮